

Effect of confining pressure on the mechanical properties of thermally treated sandstone

Feng Xu, Chunhe Yang, Yintong Guo, Tongtao Wang, Lei Wang and Ping Zhang

To understand the effect of confining pressure on the mechanical properties of thermally treated coarse sandstone, uniaxial and triaxial compression tests were conducted for six groups of thermally treated sandstone from Xujiahe Formation in southwestern China under confining pressures of 0–40 MPa. The test results indicate that 600°C is a critical threshold of the thermal damage of sandstone by SEM and mechanical tests. When temperature is below 600°C, few micro cracks are observed by SEM. Peak strength, elastic modulus, cohesion and internal friction angle remain constant or increase with increasing temperature and all these values decrease when temperature is above or equal to 600°C under different confining pressures. Under the uniaxial and low confining pressure (≤ 5 MPa), the failure mode shows single or multiple splitting planes and it is easier to generate complex cracks with increasing temperature. Under high confining pressure (10–40 MPa), the failure mode shows a simple shear plane after treatment at different temperatures, i.e. 25–1000°C. The results may provide guidance for rock engineering design after high temperature exposure.

With the rapid development of deep mining, underground, nuclear waste disposal and geothermal exploitation, the mechanical properties of rocks under different temperatures need to be studied because relevant parameters are the basic foundations for excavation of rock underground engineering, designing support, and stability analysis of the surrounding rocks at high temperature^{1–6}.

Previously, several experiments have been conducted concentrating mainly on mechanical properties of rocks under uniaxial, dynamic compression and Brazilian disc test. Table 1 summarizes previously published results. Zhang *et al.*⁷ and Liu and Xu⁸ compared stress–strain curve, compression strength, peak strain and elastic modulus of different types of rocks such as sandstone, granite and marble after high temperature exposure and found that different rocks have similar trends with regard to physico-mechanical properties. Chaki *et al.*⁹ reported an increase in the permeability of granite rock, and a decrease in compressive strength and *P*-wave velocity at higher temperatures. The overall change in the dynamic compressive strength of biotite granite is not obvious before 600°C, and above 600°C, the dynamic compressive strength decreases significantly with increasing temperature¹⁰. For sandstones, the physical properties after high temperature exposure change compared to those at room temperature. The variations can be neglected after thermal

treatment in the 100–200°C range, but normally, become significant above 400°C or 500°C (refs 8, 11, 12). Ranjith *et al.*¹³ carried out uniaxial compressive test on Hawkesbury sandstone, Sydney, Australia at various temperatures between 25°C and 950°C. They found that the uniaxial compressive strength (UCS) and elastic modulus of the sandstone increase with increasing temperature for values 500°C, and decrease with increasing temperature for values higher than 500°C. Studies have shown that due to the change in confining pressure, there is great difference in *P*- and *S*-wave velocities, compression strength and failure mode of sandstones^{14,15}. Saluja and Singh¹⁶ observed that the confining pressure has an obvious effect on the mechanical properties of rocks; for example, in the case of specimens fractured along a single oblique plane, the strength and the angle of fracture increase with the confining pressure. Zhang *et al.*¹⁷ found that both the deformation modulus and Poisson ratio increased with increase in confining pressure.

Although several researchers have studied the mechanical properties of rocks after high temperature exposure or mechanical properties of sandstone under triaxial compression tests, there are few experimental studies on post-high-temperature rocks, especially on sandstone, under triaxial compression. Thus, the main aim of this communication is to study the effect of confining pressure on

the mechanical properties of thermally treated sandstone.

Specimen preparation and test equipment

The coarse sandstones were collected from Chongqing, southwest of China. The average density of the sandstones is 2.50 g/cm³. It is composed mainly of quartz, albite, illite, kaolinite and montmorillonite. The standard cylindrical specimens with a diameter of 25 mm and length of 50 mm, were cored, cut and polished in the Institute of Rock and Soil Mechanics, Chinese Academy of Sciences following the methods suggested by International Society for Rock Mechanics¹⁸.

In order to examine the effect of temperature on the mechanical properties of sandstone under different confining pressures, the test temperature was set at six different values: 25°C (room temperature), 200°C, 400°C, 600°C, 800°C and 1000°C. At each temperature, ten specimens were heated in a furnace filled with air at a heating rate of 10°C/min. After reaching the target temperature, the specimens were maintained at that value with a standard deviation of 1°C for 60 min to make the temperature uniform in the entire specimen. The specimens were left in the furnace to cool down naturally to room temperature by turning-off the power^{8,11}.

TECHNICAL NOTES

Table 1. Mechanical properties of rocks after exposure to high temperature obtained by different researchers

	Rock type	Temperature (°C)							Reference
		25	100	200	400	600	800	1000	
Normalized elastic	Sandstone	1.00	0.90	0.75	0.50	0.54	0.30	0.20	7
	Sandstone	1.00	1.06	1.03	0.93	1.05	0.68	–	6
	Sandstone	1.00	0.86	0.72	0.94	0.78	0.33	0.42	10
	Sandstone	1.00	–	1.20	1.35	0.86	0.73	–	12
	Granite	1.00	1.20	0.82	0.55	0.10	0.05	0.04	7
	Limestone	1.00	0.96	0.87	0.85	0.91	0.18	–	6
Normalized peak strength	Marble	1.00	1.11	0.80	0.60	0.64	0.43	–	6
	Sandstone	1.00	0.83	1.03	0.97	1.03	1.03	0.22	7
	Sandstone	1.00	0.96	0.64	1.03	1.17	0.70	–	6
	Sandstone	1.00	1.13	1.05	1.23	0.98	0.97	0.93	10
	Sandstone	1.00	–	1.16	1.67	1.78	1.67	–	12
	Granite	1.00	0.94	0.98	0.96	0.83	0.67	0.36	7
Normalized <i>P</i> -wave	Limestone	1.00	0.74	0.80	0.81	0.74	0.24	–	6
	Marble	1.00	1.21	0.60	0.60	0.58	0.67	–	6
	Sandstone	1.00	0.95	0.83	0.59	0.51	0.49	0.22	7
	Granite	1.00	1.14	0.90	0.74	0.35	0.21	0.15	7



Figure 1. Photographs of sandstone specimens after high temperature exposure.

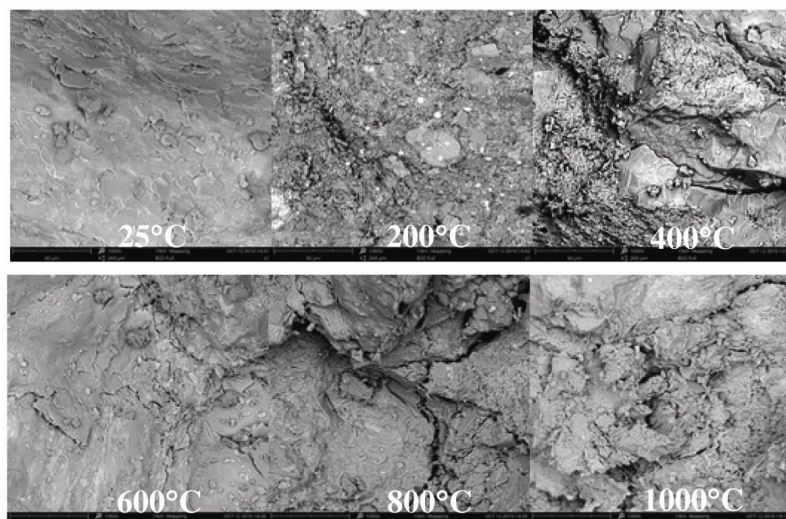


Figure 2. SEM ($\times 1000$) images of sandstone after high temperature exposure at the indicated temperatures.

All uniaxial and triaxial compression tests were conducted in the XTR01-01 servo-controlled rock mechanics testing system. This system is capable of carry-

ing out quasi-static and dynamic experiments. In tests, we measured axial load with loading capacity of 200 kN, confining pressure with loading capacity of

80 MPa, axial deformation with displacement capacity of 5 mm, and lateral chain deformation with displacement capacity of 7 mm. The loading rate was set as 0.18 mm/min under displacement control, and the axial force, confining pressure, and axial and lateral chain displacements were recorded in real time. More details regarding this set-up are given in Mao *et al.*¹⁹.

Compared with the specimen at 25°C (room temperature), the colour of the specimen at 200°C is not much different when viewed with the naked eye. From 200°C to 600°C, a notable change in colour of the specimens is observed from light grey to brownish-red. When the temperature increases from 600°C to 1000°C, the colour of the sandstone specimen becomes lighter. Figure 1 shows the change in colour of thermally treated sandstone. We observed microscopic structures by scanning electron microscope (SEM) after high temperature exposure. The results reveal that there are several micro cracks when the temperature of thermal treatment is above 600°C, however, when temperature ranges from 25°C to 400°C, there are few micro cracks in the internal structure of sandstone (Figure 2). By measuring the volume and weight of the sandstone specimens before and after different high temperature exposures, we obtained the variations in density with temperature (Table 2 and Figure 3). In general, the density of sandstone specimens after high temperature exposure shows a gradual decrease compared to room temperature.

Table 2. Test temperature, confining pressure, specimen dimension and mechanical properties

Test temperature (°C)	Specimen number	Confining pressure (MPa)	Diameter (mm)	Length (mm)	Density (g/cm ³)	Young's modulus (GPa)	Peak strength (MPa)	Cohesion (MPa)	Internal friction angle (°)
25	N-6	0	24.83	50.23	2.51	7.23	42.40	30.16	38.40
	N-1	5	24.82	50.30	2.50	8.03	77.00		
	N-2	10	24.89	50.23	2.50	8.91	94.83		
	N-3	20	24.86	50.29	2.49	11.04	137.85		
	N-4	30	24.86	50.27	2.49	13.43	177.91		
	N-5	40	24.81	50.34	2.51	16.07	219.09		
200	A-1	0	24.57	50.18	2.48	7.50	41.06	33.27	40.25
	A-2	5	24.77	50.02	2.42	8.35	78.18		
	A-3	10	25.23	50.21	2.49	9.91	132.67		
	A-4	20	24.77	50.02	2.44	12.73	145.61		
	A-5	30	24.72	50.20	2.43	15.59	198.36		
	A-6	40	24.79	50.10	2.43	17.73	238.73		
400	B-6	0	24.72	49.93	2.45	9.04	53.00	36.61	39.57
	B-1	5	24.78	50.00	2.45	8.83	83.31		
	B-2	10	24.82	50.25	2.51	10.81	124.96		
	B-3	20	24.63	50.17	2.41	12.36	153.55		
	B-4	30	24.73	50.09	2.48	16.84	199.01		
	B-5	40	24.74	50.24	2.45	18.89	239.60		
600	C-6	0	25.13	50.18	2.38	9.53	75.76	40.94	47.12
	C-1	5	25.05	50.37	2.44	12.73	118.34		
	C-2	10	24.71	50.18	2.46	16.59	167.49		
	C-3	20	25.37	50.21	2.38	18.49	226.78		
	C-4	30	24.98	50.07	2.46	24.80	285.87		
	C-5	40	24.77	50.19	2.43	25.73	338.66		
800	D-6	0	25.32	50.08	2.37	8.43	60.13	29.43	46.37
	D-1	5	24.77	50.21	2.33	6.67	81.27		
	D-2	10	24.65	50.25	2.33	11.13	133.13		
	D-3	20	24.72	50.10	2.35	12.07	189.73		
	D-4	30	25.30	50.14	2.38	18.09	265.26		
	D-5	40	24.68	50.22	2.38	21.30	297.32		
1000	E-6	0	24.83	50.27	2.36	5.20	40.54	26.39	39.26
	E-1	5	24.82	50.32	2.35	5.72	66.04		
	E-3	10	24.85	50.10	2.30	7.46	85.79		
	E-4	20	24.80	50.04	2.35	9.97	141.92		
	E-5	30	24.82	50.05	2.38	12.21	190.76		
	E-7	40	24.83	50.07	2.35	12.91	209.87		

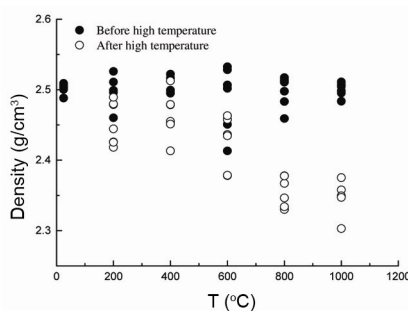


Figure 3. Variations in density before and after high temperature (T) exposure.

Experimental results and analysis

The differential stress–strain curve of sandstone is a direct reflection of its mechanical properties. It shows variation of

the mechanical properties of sandstone under different confining pressures after high temperature exposure (Figure 4 and Table 2). The specimens go through phases of compaction, elastic deformation, yield and failure. Significant differences in the mechanical properties are noticed at different confining pressures after high temperature exposure.

Variation of peak strength

The relationship between peak strength and temperature can be divided into three stages. First, between 25°C and 400°C, the peak strength rises slowly with increase in temperature. Second, between 400°C and 600°C, peak strength increases sharply. Lastly, the peak strength begins to decrease above 600°C. When the tem-

perature increases from 25°C to 1000°C, the average peak strength at different confining pressures increases by 11%, 16%, 65%, 35% and –4% respectively (Figures 5 and 6). By regression analysis, the mean normalized peak strength (MNPS) of thermally treated sandstone under different confining pressures and temperature satisfies the following equation

$$MNPS = -5\left(\frac{T}{1000}\right)^3 + 5\left(\frac{T}{1000}\right)^2 + 1.021 (R^2 = 0.836), \quad (1)$$

where MNPS represents the mean value of normalized peak strength under different confining pressures, T the temperature of thermally treated sandstone and R is the relative coefficient. We assume that the normalized peak strength (NPS) is

1.0 at room temperature under different confining pressures; so NPS can be calculated after high temperature exposure (Figure 6).

Figure 7 shows the relationship between peak strength and confining pressure after exposure of the sample to different high temperatures. The peak strength increases with increasing confining pressure; there is a linear relation with the confining pressure. The rate of increase is different for exposure of the sample to different high temperatures. When the confining pressure increases from 0 to 40 MPa, increasing peak strength for 25°C, 200°C, 400°C, 600°C, 800°C and 1000°C is 417%, 481%, 352%, 347%, 394% and 418% respectively.

Variation of cohesion and internal friction angle

As mentioned earlier, the peak strength has a linear relation with the confining

pressure after different high temperature exposures. The main type of failure modes of sandstone specimen is macro shear fracture, which follows Mohr–Coulomb failure criterion. The relationship between cohesion (c), internal friction angle (ϕ) and temperature based on the Mohr–Coulomb criterion can be expressed in terms of the peak strength σ_1 and the confining pressure σ_3 as follows²⁰

$$\sigma_1 = m\sigma_3 + b, \tag{2}$$

where m and b are coefficients and can be obtained by linear fitting and are related to cohesion and the internal friction angle as

$$\phi = \arcsin \frac{m-1}{m+1}, \tag{3}$$

$$c = \frac{b(1 - \sin \phi)}{(2 \cos \phi)}, \tag{4}$$

Figure 7 shows the influence of confining pressure on peak strength for sandstone specimens in accordance with eq. (2). When temperature ranges from 25°C to 1000°C, there are good linear regression coefficients of $R = 0.995$, $R = 0.957$, $R = 0.983$, $R = 0.989$, $R = 0.985$ and $R = 0.982$. Cohesion and internal friction angle can be calculated according to eqs (2)–(4). Figure 8 shows the relationship between c , ϕ and temperature. c ranges from 26.39 to 40.94 MPa and ϕ ranges from 38.40° to 47.12°. The cohesion increases at first and then decreases with increasing temperature. It increases almost linearly from 30.16 to 40.94 MPa with the temperature ranging from 25°C to 600°C. When the temperature exceeds 600°C, cohesion decreases with further increase in temperature. Also, cohesion decreases to a minimum of 26.39 MPa when the temperature reaches 1000°C. However, the variation of the internal friction angle was low. When temperature ranges from 25°C to 400°C, remains almost constant. When temperature increases from 400°C to 600°C, its increases sharply and reaches a maximum of 47.12°. When the

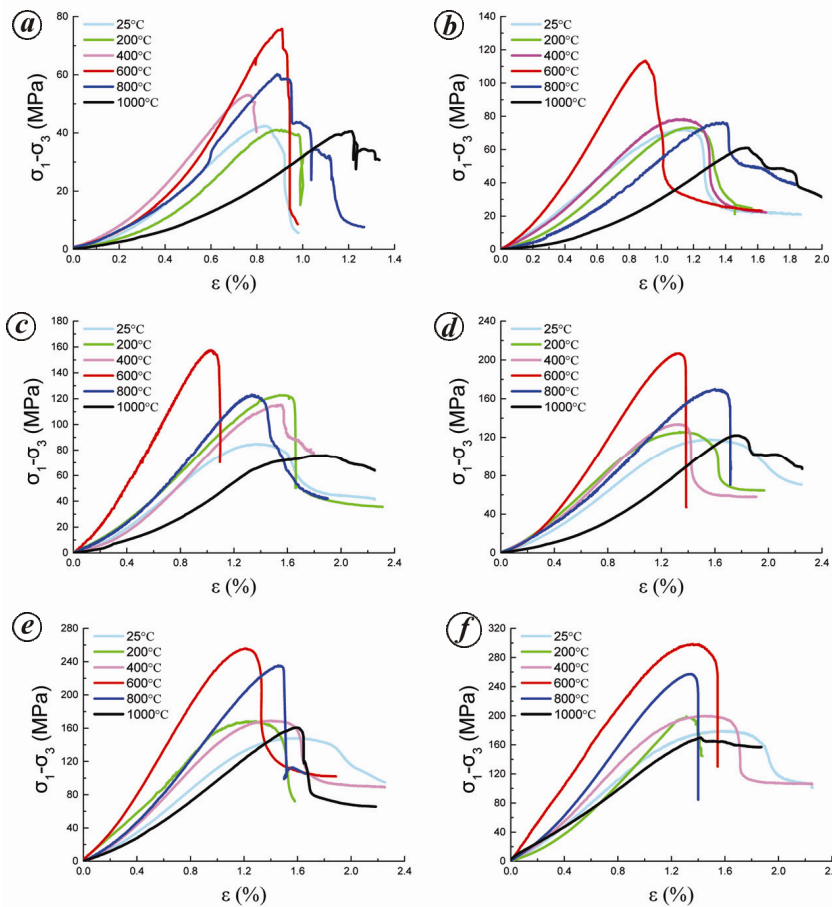


Figure 4. Stress–strain curves of sandstone under different confining pressures after high temperature exposure. (a) 0 MPa; (b) 5 MPa; (c) 10 MPa; (d) 20 MPa; (e) 30 MPa; (f) 40 MPa.

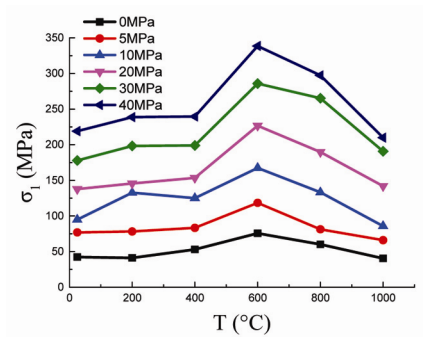


Figure 5. Relationship between peak strength (σ_1) and temperature (T) to which the sandstone has been exposed.

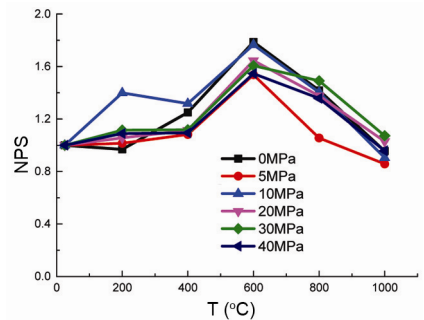


Figure 6. Relationship between normalized peak strength (NPS) and treatment temperature (T) of sandstone.

temperature increases from 600°C to 1000°C, the internal friction angle decreases from 47.12° to 39.26°.

Variation of elastic modulus

In this study elastic modulus represents the slope corresponding to 40% and 60% of peak strength during the rising phase of the stress–strain curve. Figure 9 presents the relationship between elastic modulus and confining pressure. When the confining pressure increases from 0 to 40 MPa, the elastic modulus increases by 122%, 136%, 109%, 170%, 153% and 148% when the temperature is set as 25°C, 200°C, 400°C, 600°C, 800°C and 1000°C respectively. Figure 10 shows that when the temperature ranges between 25°C and 400°C, elastic modulus of the sandstone remains constant. When the temperature ranges between 400°C and 600°C, the elastic modulus increases sharply for triaxial compression tests, but increases only a little for uniaxial compression tests. The elastic modulus starts decreasing when the temperature exceeds 600°C.

Variation of failure mode

In accordance with the failure mode of sandstone shown in Figure 11, in this study the specimens show typically axial splitting failure under uniaxial compression, and shear failure under triaxial compression tests. When the confining pressure is below or equal to 5 MPa, the failure mode of sandstone specimens gradually becomes complicated as the temperature increases. Taking the uniaxial compression (confining pressure is zero) tests for example, when temperature falls between 25°C and 400°C, the failure mode shows single or multiple splitting planes. Above 400°C, the

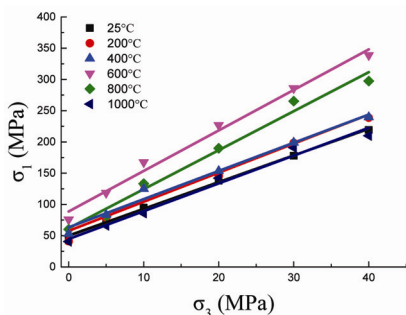


Figure 7. Relationship between peak strength (σ_1) and confining pressure (σ_3).

failure mode shows many cracks and multiple intersecting failure planes. When confining pressure ranges from 10 to 40 MPa, the failure mode shows a simple shear plane after different high temperature treatments.

Discussion

When treatment temperature is below 400°C, both peak strength and elastic modulus change a little with increasing temperature under different confining pressures. This could be attributed to the fact that the crystal and absorbed water

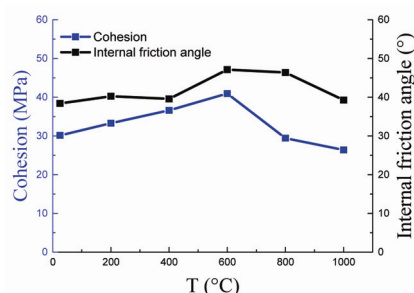


Figure 8. Relationship between cohesion (c), internal friction angle ϕ and temperature.

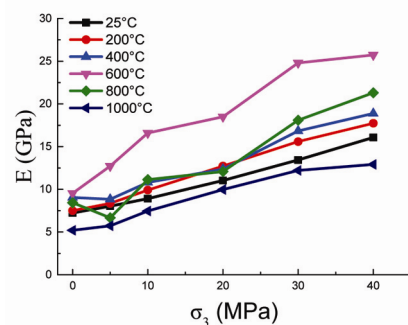


Figure 9. Relationship between elastic modulus (E) and confining pressure.

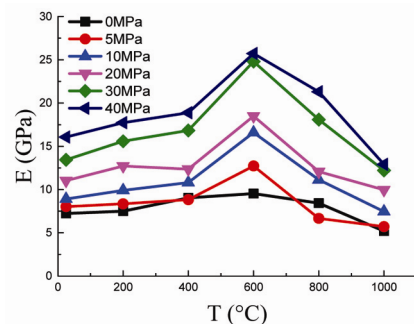


Figure 10. Relationship between elastic modulus (E) and temperature (T).

of minerals would escape from the internal mineral structure, but the original fissures and pore structure of the sandstone remain unchanged. When the treatment temperature falls between 400°C and 600°C, the peak strength and elastic modulus increase sharply. This can be explained by the fact that the number of original cracks is reduced because of partial melting and recrystallization of minerals such as montmorillonite and kaolinite, in the original cracks, which results in thermally induced strengthening, as observed by Ranjith *et al.*¹³ and Wu *et al.*²¹. When treatment temperature is above 600°C, both peak strength and elastic modulus decrease with increase in temperature because a large number of micro cracks are generated in the sandstone as revealed by SEM (Figure 2), due to the different thermal expansion coefficients of minerals. When confining pressure is below or equal to 5 MPa, the failure mode shows single or multiple splitting planes; this result is also supported by previous studies. It is easier to generate complex cracks as the temperature increases. Taking the uniaxial compression tests for example, when temperatures fall between 25°C and 400°C, the failure mode shows single or multiple splitting planes. Above 600°C, the failure mode shows many cracks and multiple intersecting failure planes. This could be attributed to interior structures being damaged when temperature is above or equal to 600°C. The failure mode shows a simple shear fracture because high confining pressure can effectively close cracks induced by thermal damage and restrain the formation of splitting planes at confining pressures over 5 MPa.

Conclusion

Based on the results obtained, it can be concluded that confining pressure has an obvious effect on mechanical properties of thermally treated sandstone specimens. The main conclusions are summarized below.

- (1) Experimental results suggest that 600°C is the critical threshold of thermal damage of sandstone for both uniaxial and triaxial compression tests. When temperature is below 600°C, few micro cracks are observed by SEM, and peak strength, elastic modulus, cohesion and internal friction angle remain constant or

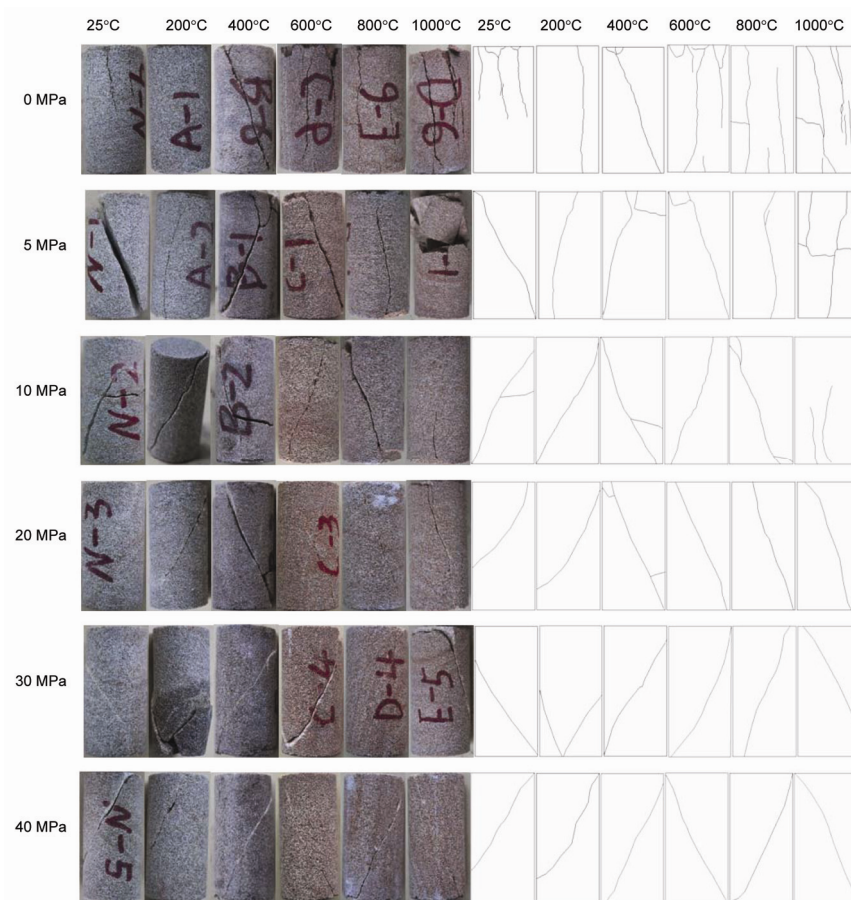


Figure 11. Failure mode of sandstone specimens.

increase, but some micro cracks come into being and all these values decrease when temperature is above 600°C.

(2) Peak strength and elastic modulus increase with increase in confining pressure of sandstone after different thermal treatments, but the growth rates are different.

(3) When confining pressure is below or equal to 5 MPa, the failure mode shows single or multiple splitting planes and it is easier to generate complex cracks as the temperature increases. When confining pressure is over 5 MPa, the failure mode shows a simple shear fracture.

1. Wong, T. F., *Mech. Mater.*, 1982, **1**, 3–17.
 2. Wai, R. S. C. and Lo, K. Y., *Can. Geotech. J.*, 1982, **19**(3), 307–319.

3. Zhang, Z. X., Yu, J., Kou, S. Q. and Lindqvist, P. A., *Int. J. Rock Mech. Min. Sci.*, 2001, **38**(2), 211–225.
 4. Kanagawa, K., Cox, S. F. and Zhang, S. Q., *J. Geophys. Res. – Solid Earth*, 2000, **105**(B5), 1115–11126.
 5. Baud, P., Wong, T. F. and Zhu, W., *Int. J. Rock Mech. Min. Sci.*, 2014, **67**(4), 202–211.
 6. Misra, S. et al., *J. Geophys. Res. – Solid Earth*, 2014, **119**(5), 3971–3985.
 7. Zhang, L., Mao, X. and Lu, A., *Sci. China Ser. E*, 2009, **52**(3), 641–646.
 8. Liu, S. and Xu, J., *Eng. Geol.*, 2015, **185**, 63–70.
 9. Chaki, S., Takarli, M. and Agbodjan, W. P., *Constr. Build. Mater.*, 2008, **22**(7), 1456–1461.
 10. Liu, S. and Xu, J., *Int. J. Rock Mech. Min. Sci.*, 2014, **71**, 188–193.
 11. Wu, G., Wang, Y., Swift, G. and Chen, J., *Geotech. Geol. Eng.*, 2013, **31**(2), 809–816.

12. Tian, H., Kempka, T., Xu, N.-X. and Ziegler, M., *Rock Mech. Rock Eng.*, 2012, **45**(6), 1113–1117.
 13. P. G. R. Viete, D. R., Chen, B. J. and Perera, M. S. A., *Eng. Geol.*, 2012, **151**, 120–127.
 14. Klein, E., Baud, P., Reuschle, T. and Wong, T. F., *Phys. Chem. Earth Part A*, 2001, **26**(1–2), 21–25.
 15. Dillen, M. W. P., Cruts, H. M. A., Groenenboom, J., Fokkema, J. T. and Duijndam, A. J. W., *Geophysics*, 1999, **64**(5), 1603–1607.
 16. Saluja, S. S., Singh, D. P. and Kasiviswanadham, M., *J. Mines, Met. Fuels*, 1977, **25**(5), 131–138.
 17. Zhang, H., Kang, Y., Chen, J., Han, L. and Wang, Y., *Chin. J. Rock Mech. Eng. (Suppl. 2)*, 2007, **26**, 4227–4231.
 18. Deutsch, *The ISRM Suggested Methods for Rock Characterization, Testing and Monitoring: 2007–2014* Springer. Springer International Publishing, 2015.
 19. Mao, H. J., Yang, C. H. and Liu, J., *Chin. J. Rock Mech. Eng.*, 2006, **25**(6), 1204–1209.
 20. Yang, S. Q., Jiang, Y. Z., Xu, W. Y. and Chen, X. Q., *Int. J. Solids Struct.*, 2008, **45**(17), 4796–4819.
 21. Wu, G., Xing, A. and Zhang, L., *Chin. J. Rock Mech. Eng.*, 2007, **26**(10), 2110–2116.

ACKNOWLEDGEMENTS. We thank Prof. J. J. K. Daemen (University of Nevada, USA) for help with language and the National Natural Science Foundation of China (No. 51574218, No. 51621006, No. 41602328) and Youth Innovation Promotion Association CAS (No. 2016296) for financial support.

Received 1 August 2016; revised accepted 27 December 2016

Feng Xu*, Chunhe Yang, Yintong Guo, Tongtao Wang and Lei Wang are in the State Key Laboratory of Geomechanics and Geotechnical Engineering, Institute of Rock and Soil Mechanics, Chinese Academy of Sciences, Wuhan 430071, Hubei, China; Feng Xu is also in the University of Chinese Academy of Sciences, Beijing 100049, China; Chunhe Yang and Ping Zhang are also in the State Key Laboratory of Coal Mine Disaster Dynamics and Control, Chongqing University, Chongqing 400044, Chongqing, China.
 *e-mail: ucasxf@163.com